MEASURED AND SIMULATED FLOW NEAR SPUR DIKES

Roger A. Kuhnle[1], Yafei Jia[2], and Carlos V. Alonso[3]

ABSTRACT.

To improve understanding of the flow and scour processes associated with spur dikes more fully, 3-dimensional flow velocities were measured using an acoustic Doppler velocimeter at a closely spaced grid over a fixed flat bed and a fixed scoured bed with a submerged trapezoidal shaped spur dike. Flow velocities were measured at 2592 points for the flat bed and 3484 points for the scoured bed in the vicinity of the spur dike and the scour hole. General distribution of velocities and detailed near field flow structures were revealed by the measurements. Some important differences between the flow fields measured in this study and those measured for non-submerged vertical obstructions were observed in this study. Numerical simulation was performed using the free surface turbulent flow model, CCHE3D. The numerical simulation of the flow velocity field generally showed very good agreement between the computation results and the measurements. Bed shear stress fields derived from measured and simulated data showed some discrepancies. The numerical simulation results indicate the CCHE3D model can be used to reasonably predict near-field flows around hydraulic structures; however, further research is needed for accurate prediction of local scour using simulated flows.

1. INTRODUCTION

A spur dike may be defined as a structure extending outward from the bank of a stream for the purpose of deflecting the current away from the bank to protect it from erosion. In many instances impaired streams and rivers often erode the banks and move laterally, resulting in land loss, channel change, excessive sediment yield and degradation of the water quality. The use of a series of spur dikes is one of the most effective means of stabilizing or realigning channel banks. For economic reasons, spur dikes are often constructed of riprap and are commonly designed to be submerged during high flows. The pools formed from the local scour associated with spur dikes have been used successfully to enhance aquatic habitat in unstable streams (Shields et al., 1995). Despite the widespread use of spur dikes, many aspects of their design are based on prior experience and are

[1]Research Hydraulic Engineer, Channel and Watershed Processes Research Unit, National Sedimentation Laboratory , U.S. D. A. Agricultural Research Service, P. O. Box 1157, Oxford, MS 38655, USA. Phone: 1-(662)-232-2971 Fax: 1-(662)-281-5706 Email: rkuhnle@msa-oxford.ars.usda.gov
[2] Research Associate Professor, National Center for Computational Hydroscience & Engineering, The University of Mississippi, Carrier Hall Room 102, P.O. Box 1848, University, MS 38677-1848. Phone: 1-(662)-915-7783 Fax: 1-(662)-915-7796 Email: jia@ncche.olemiss.edu
[3]Research Leader, Channel and Watershed Processes Research Unit, National Sedimentation Laboratory , U.S. D. A. Agricultural Research Service, P. O. Box 1157, Oxford, MS 38655, USA. Phone: 1-(662)-232-2969 Fax: 1-(662)-281-5706 Email: calonso@msa-oxford.ars.usda.gov

only applicable to streams of a similar nature (Copeland, 1983). An improved understanding of the complicated 3-D flow in the vicinity of spur dikes and its interaction with the entrainment and transport of sediment is needed.

There have been few previous studies of the flow in the vicinity of spur dikes. Rajaratnam and Nwachukwu (1983) studied the flow in a laboratory flume near groin-like structures represented by an aluminum plate which projected above the water surface. A pitot-static tube was used to measure the flow in regions of undisturbed flow and a three-tube yaw probe was used in regions of skewed flow. They found that the bed shear stresses at the upstream corner of the plate were up to five times the bed shear stresses in the approach flow section. The initiation of local scour is associated with the increase in shear stress caused by the accelerating flow around the obstruction. For cylindrical bridge piers, scour has been observed to be dominated by a strong downflow on the upstream side of the pier and a horseshoe vortex which surrounds the upstream and lateral sides of the pier (e.g. Mellville and Raudkivi, 1977; Graf and Yulistiyanto, 1998; Istiyato and Graf, 2001). For bridge abutments, which are in many ways similar to spur dikes, flow features resembling those observed around one-half of a cylindrical bridge pier have been measured, including the primary vortex (essentially one half of the horse-shoe vortex), which forms around the structure and contributes to the development of scour (Kwan and Melville, 1994). These investigators have concluded that the flow structures around a model wingwall abutment are dominated by the large primary vortex and an associated downflow.

Detailed velocity measurements around a submerged spur dike with a trapezoidal shape are rare. Flow around this structure would be expected to vary from that of flat plates and abutments due to the over-topping flow and 3-dimensional shape of the structure. The over-topping flow and trapezoidal shape would be expected to affect the characteristics of the primary vortex and make the recirculation zone behind the spur dike more three-dimensional. Because the flow is the key to understanding the performance of a submerged spur dike, the velocity field around the spur dike was measured in a laboratory flume at the National Sedimentation Laboratory. The data sets of 2592 point measurements on the fixed flat bed and 3484 point measurements on the fixed scoured bed were compared to flow simulations calculated using the 3-dimensional numerical flow model (CCHE3D) developed at the National Center for Computational Hydroscience and Engineering, University of Mississippi. The distribution of bed shear stresses derived from measured and simulated flows were used to predict the location of local scour adjacent to the spur dike.

2. PHYSICAL MODEL AND VELOCITY DATA

All of the flow measurements were collected in a recirculating flume with a test channel 30 m long, 1.2 m wide, and 0.6 m deep located at the National Sedimentation Laboratory. Flow rate in the flume was measured using a pressure transducer connected to a Venturi meter in the return pipe. Flow depth was controlled by the amount of water in the flume and measured by taking the difference in elevation between 12-m long bed and water surface transects in the approach flow section. The bed of the approach flow section was covered with sediment (D_{50} = 0.8 mm, $[D_{84}/D_{16}]^{1/2}$ =1.35). The bed sediment was immobilized with a thin layer of cement from 21.9 m downstream of the channel inlet to the tail box to prevent the bed from changing. The zero location of the *x* (streamwise) coordinate was located 22.6 m downstream of the channel inlet and the center of the spur dike model was located 1.19 m downstream from the zero coordinate. The spur dike model (Fig. 1) was located on the left wall of the channel facing downstream. Flow conditions were very similar to those used in one experiment from Kuhnle, et al. (1999) and are summarized in Table 1. The ratio of the bed shear velocity to the critical bed shear velocity of the bed material sediment, obtained from a modified Shields curve (Miller et al., 1977), was 0.7 in the approach flow section.

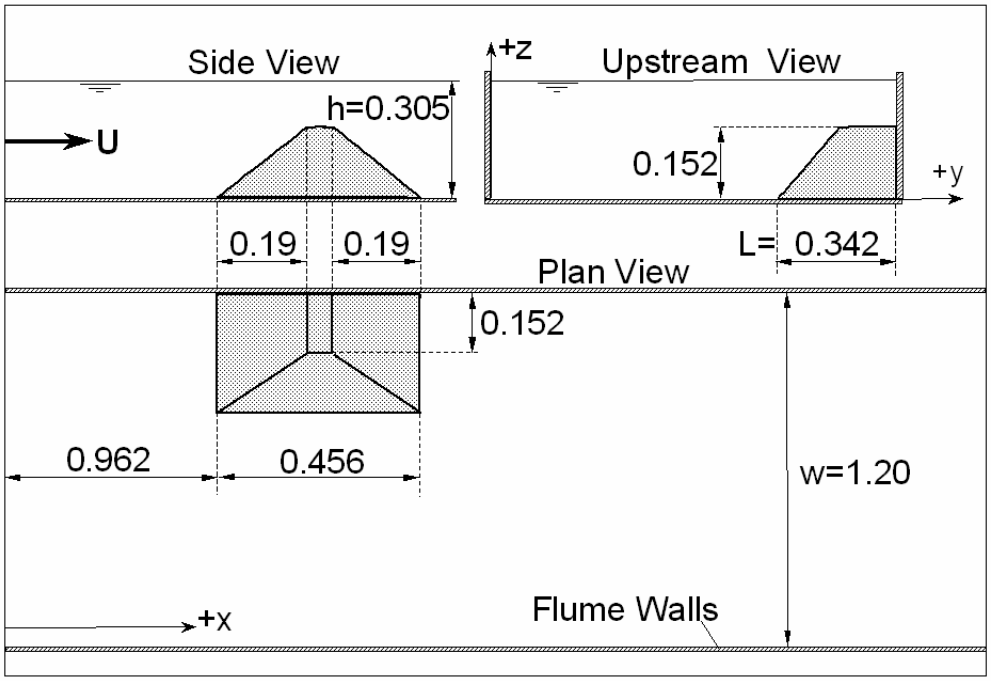

Figure 1. Definition sketch of experimental setup. The shaded block represents the model spur-dike. All dimensions are in meters. The coordinate convention used was x – streamwise direction, y – cross stream, z - vertical, with the origin at the upstream right wall on the bed of the channel. h is defined as the flow depth upstream of the structure. Channel width is not to scale with other dimensions.

Table 1. Flow condition of the flume experiments.

Exp. Run	Flow rate (m^3/s)	Flow depth (m)	Mean Flow velocity (m/s)	Froude Number
Flat fixed bed	0.129	0.3048	0.347	0.201

The velocity data was collected using a commercially available Acoustic Doppler Velocimeter (ADV). The measurement head of the ADV is mounted on a stainless steel mast 60 cm long and 1 cm in diameter. The measurement head has three sensors mounted at a spacing of 120^o around a circle approximately 7 cm in diameter. The sampling volume of the ADV (170 mm^3) is a cylinder 6 mm in height and 6 mm in diameter, located 5 cm away from the head of the ADV. Flow velocity data at each point was collected at 50 Hz for 5 minutes. The 5 minute sample duration was determined empirically as the optimum length of time to capture the mean velocity and turbulence quantities at the sampling locations within a reasonable time frame.

Flow velocities were measured at 288 locations as shown in Figure 2. At each location for the flat fixed bed, the flow was measured at 9 vertical positions: 0.0100, 0.0225, 0.0350, 0.0475, 0.0600, 0.1000, 0.1400, 0.1800, and 0.2200 m above the bed. In the scoured bed experiments the same grid of 288 locations was maintained, however, where the bed had been scoured (Fig. 3), flow measurements were also made at 0.25 cm below the pre-scoured bed elevation and at 1.25 cm intervals for as many measurements as possible down to the bed. This resulted in from 9 to 19 measurements in the vertical for each position. The vertical measurement positions were adjusted accordingly at the locations above the spur dike to arrive at nine measurement positions. A total of

2592 and 3484 velocity vectors were measured over the fixed flat and scoured beds, respectively. All velocity records were processed using the public domain program, WinADV. Measurements were filtered using WinADV to reject points with a correlation coefficient less than 0.7. In most files less than 10% of the correlation coefficients were rejected.

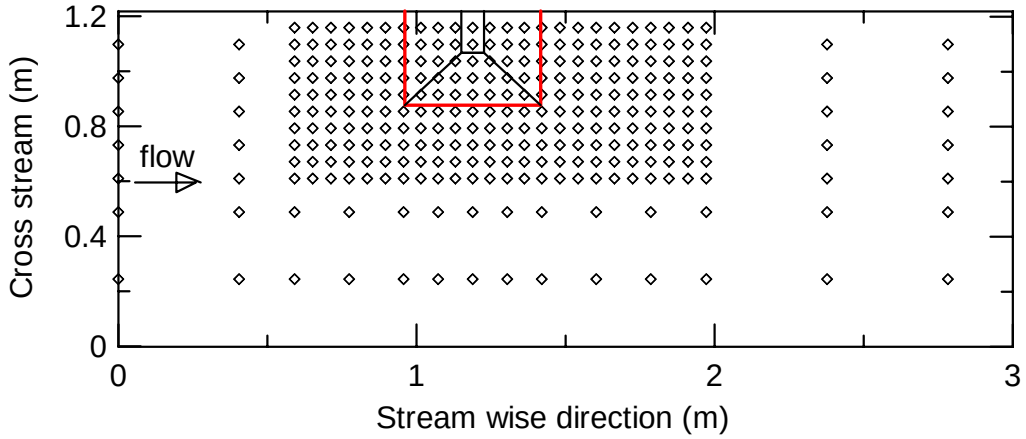

Figure 2. Plan view of experimental flume with measurement locations indicated by diamond symbols. Outline of base of spur dike shown in red.

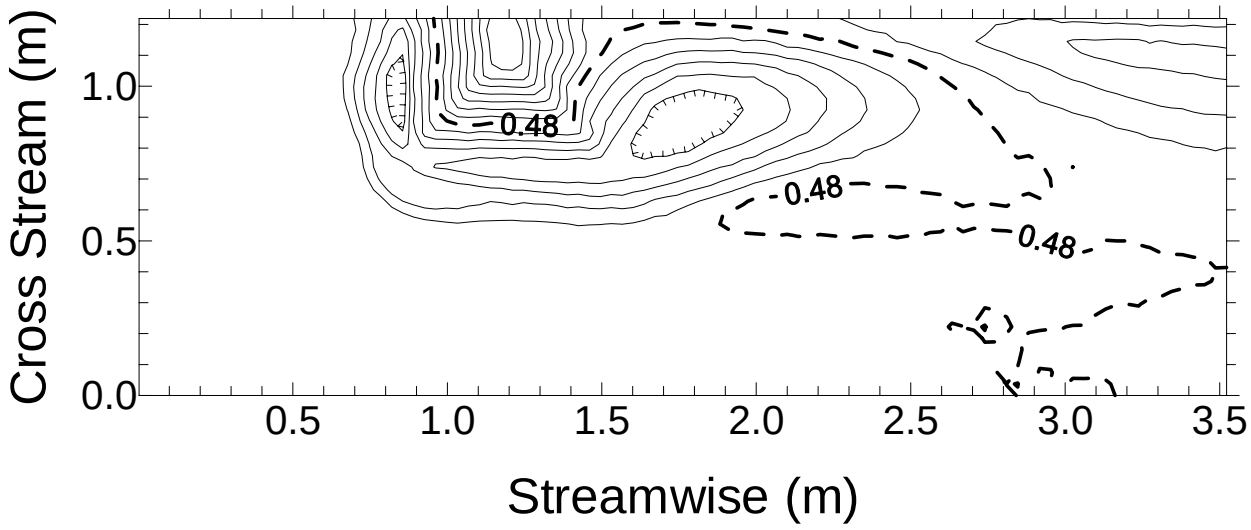

Figure 3. Topographic map of scoured fixed bed. Bed was allowed to scour for 30 hours before it was fixed with a thin layer of cement. Contour interval is 0.02 m.

3. NUMERICAL SIMULATION MODEL

Numerical simulations of three-dimensional free surface flow around hydraulic structures have been attempted with reasonable success (Jia and Wang 1996, 1999, Richardson, and Punchang, 1998). The three-dimensional, unsteady, turbulent free surface flow model CCHE3D, has been applied to simulate the flow around submerged spur dikes in this study. This model has been applied (Jia and Wang, 2000) to simulate a similar experimental case conducted by Kuhnle et al. (1997), to study flow field and local scouring without measured velocity data. This model uses the finite element method to solve the following governing equations.

The Reynolds stress equations:

$$u_{i,t} + u_j u_{i,j} - (-\overline{u_i u_j})_{,j} + \frac{p_i}{\rho} + f_i = 0 \tag{1}$$

$$u_{j,j} = 0 \tag{2}$$

where u represents the mean velocity, u' represents the turbulent velocity fluctuation, p is the mean pressure, ρ is the density of the water, and f is the gravitational force.

The free surface kinematic equation:

$$\frac{\partial \eta}{\partial t} + u_\eta \frac{\partial \eta}{\partial x} + v_\eta \frac{\partial \eta}{\partial y} + w_\eta = 0 \tag{3}$$

where η denotes the free surface elevation.

The k-ε turbulence closure scheme:

$$k_{,t} + u_j k_{,j} - (\frac{\nu_k}{\sigma_k} k_{,j})_{,j} = P - \varepsilon \tag{4}$$

$$\varepsilon_{,t} + u_j \varepsilon_{,j} - (\frac{\nu_k}{\sigma_\varepsilon} \varepsilon_{,j})_{,j} = c_{\varepsilon 1} P \frac{\varepsilon}{k} - c_{\varepsilon 2} \frac{\varepsilon}{k^2} \tag{5}$$

where k represents the turbulent kinetic energy $u_i' u_i'/2$, ε represents the rate of dissipation of turbulent kinetic energy, ν_t denotes the turbulent viscosity given by:

$$\nu_t = c_\mu \frac{k^2}{\varepsilon} \tag{6}$$

and P is the production of turbulent kinetic energy computed from:

$$P = \nu_t (u_{,j} + u_{,i}) u_{,i} \tag{7}$$

The values of empirical coefficients appearing in the preceding equations were assigned: σ_k=1.0, σ_ε=1.3, $c_{\varepsilon 1}$=1.44, $c_{\varepsilon 2}$=1.92, c_μ=0.09.

The velocity correction method was used to solve the momentum equations (Jia et al, 2001). A Poisson's equation formulated with the velocity correction terms and the continuity equation was solved on a staggered grid to obtain the dynamic pressure and force the flow to satisfy the divergence free condition. Wall boundary conditions were used for the momentum equations and the k-ε closure model. The shape of the spur dike is trapezoidal in both cross-sectional and longitudinal directions with very steep slopes, a body fitted 3D grid was generated over the dike. The system of equations was solved implicitly by using the SIP method with the first order Euler's scheme.

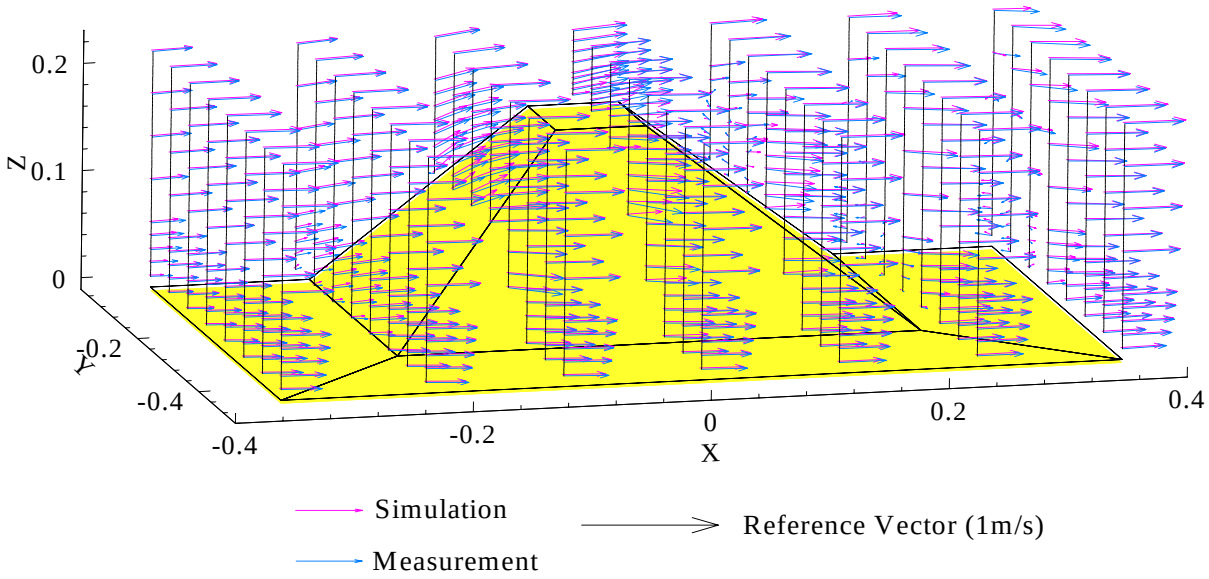

Fig. 4. A perspective view of simulated and measured flow field around the submerged spur dike.

4. SIMULATION RESULTS

Figure 4 shows a perspective view of the trapezoidal-shaped spur dike and the simulated and measured velocities in this study. The far side (Y=0) indicates the location of the vertical flume wall, and the horizontal plane is the channel bed. To focus attention and make the comparison clear, the area shown in the figure is only the close vicinity of the spur dike, and all other measured locations are ignored. The spur dike (Fig. 4) is surrounded by a field of measured and computed velocity vectors, with all the data in the seven cross sections displayed. Two velocity vectors are drawn at each point along a vertical line. The vectors in blue represent measured velocities and those in red represent the simulated velocities at the same location. Because the spatial locations of measuring points differ from mesh points of the computation, linear interpolation was applied to estimate the simulated velocity at the measuring locations. Generally, the flow field of the physical model is well reproduced by the numerical simulation. The velocity magnitude and direction of most simulated vectors agree with those measured. It is noted though, larger differences appear at several places: the corner near the wall and bed in the upstream side; in the recirculation zone downstream of the spur dike, and on the upper part of the spur dike slopes.

The simulation results were also compared to the flow measurements made over the scoured bed. In regions where the flow field was mildly accelerating or decelerating, such as to the side of the structure (Fig. 5, bottom), the agreement between measured and simulated was generally good. In regions of flow separation, such as in the lee of the spur dike, the agreement between measured and simulated values shows larger discrepancies (Fig. 5, top and middle), however, the values in the scour hole, especially near the bed, were closely predicted by the model results.

The computed and measured total velocity magnitude are depicted in Figure 6. The diagonal line represents the perfect agreement. It can be seen that the numerical prediction reproduced the physical model data with very little systematic error (r^2=0.97). The error norm for the total velocity

$$\sigma = \frac{1}{N}\sum\sqrt{\left|U_s^2 - U_m^2\right|} \approx 0.0825 \tag{8}$$

is reasonably small with U_s and U_m representing simulated and measured total velocity and N=2592 for the flat fixed bed. The point scattering is slightly higher for smaller velocities (<0.3m/s). Most of the points which scatter farther away from the diagonal line are those close to the bed or spur dike surface. This scattering reflects the possible difficulty of measuring acoustic data close to a solid surface.

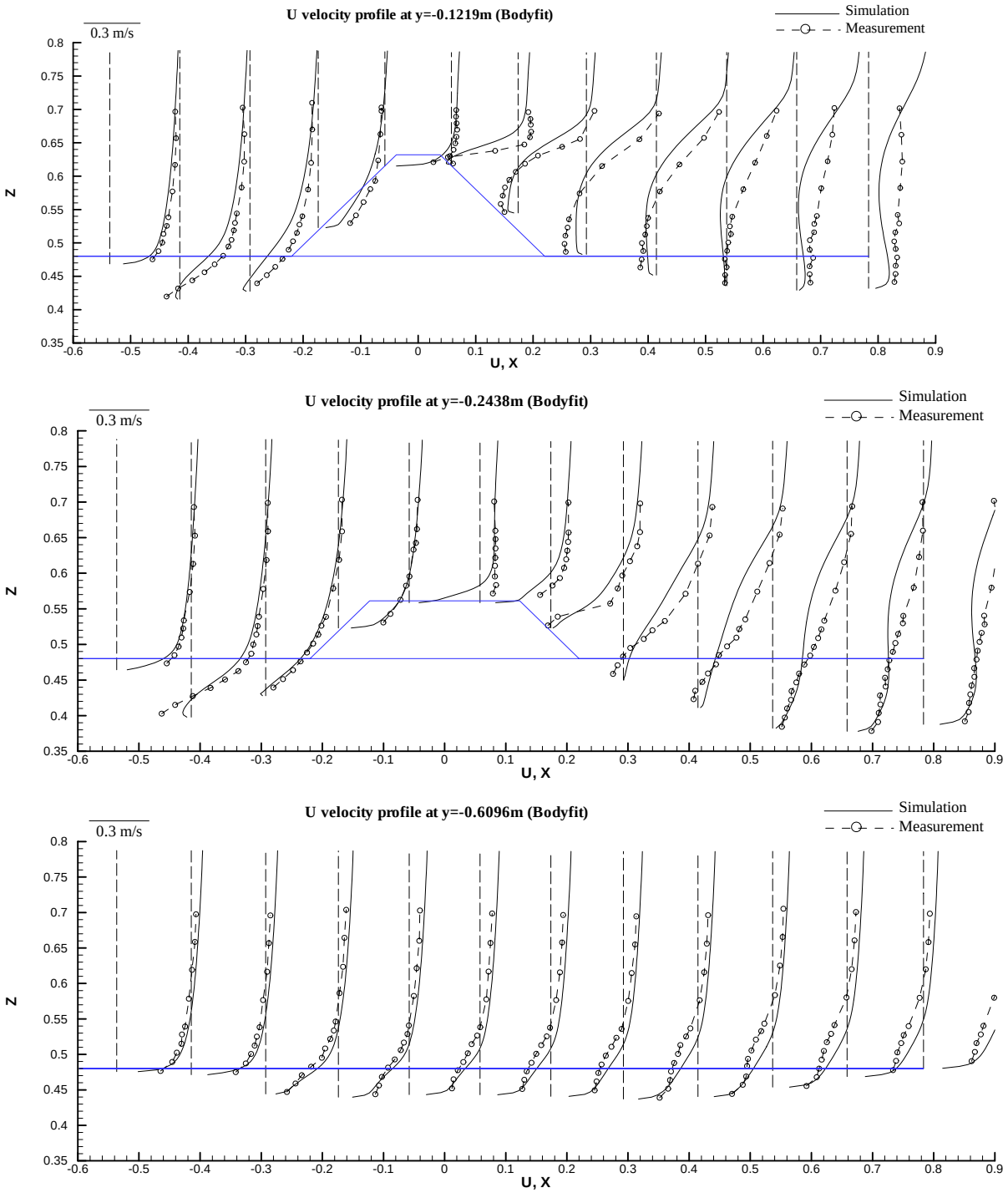

Figure 5. Comparison in streamwise direction between measured and simulated velocities for scoured bed. Top: XZ plane 1.097 m from right wall viewed downstream. Middle: XZ plane 0.9754 m from right wall viewed downstream. Bottom: XZ plane 0.6096 m from right wall viewed downstream. Blue line indicates position of prescoured sediment bed and outline of spur dike.

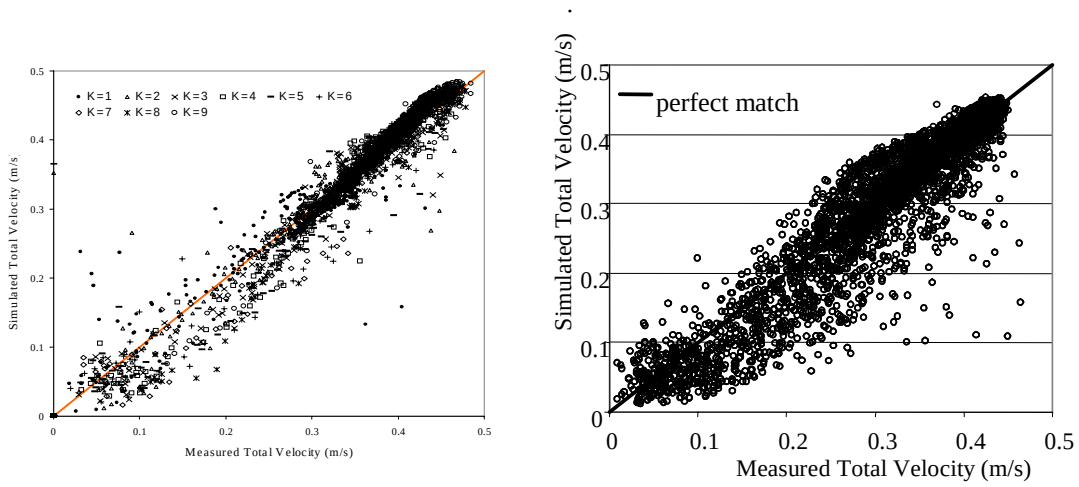

Figure. 6. Comparison of the simulated and measured total velocity magnitude. Left - relation for fixed flat bed, and right - relation for fixed scoured bed.

The comparison of the measured and predicted total velocity for the scoured fixed bed is also generally without bias for the greater magnitude flow velocities, however, flow velocities with lower magnitudes tend to be under predicted. Scatter is also significantly greater than for the flat bed case.

5. BOUNDARY SHEAR STRESS

Boundary shear stresses derived from measured and simulated velocities were compared as an indicator of the ability to predict the location and extent of local scour in the vicinity of a spur dike. For the measured flow data, linear relations were fit to Reynolds-stress profiles near the bed and extrapolated to the bed surface yielded the bed-shear stress components from the measured flow data for the flat fixed bed measurements:

$$\tau_{0ij} / \rho = - rms\left(u_i' u_j'\right)\Big|_{z=0} \tag{9}$$

Predicted shear stress values were calculated using the simulated mean velocity ($\bar{u}_i$) nearest to the boundary with the equation:

$$\frac{u}{u_*} = \frac{1}{\kappa} \ln\left(\frac{z}{z_0}\right) \tag{10}$$

where z is the distance from the wall or bed, u is the total velocity parallel to the boundary, and z_0 is the zero velocity level which was calculated with different formulas for different flow conditions of hydraulically smooth, transition, or rough conditions (see van Rijn, 1993, p. 2.4). Equation (10) was solved for u_* ($=(\tau_0 / \rho)^{1/2}$). Contour maps of the bed shear stress magnitudes normalized by critical shear stress for k_s=0.8 mm sand are presented in Figure 7. The shear stress values derived from the simulated results are greater (up to 1.7 times) in value than those derived from measured velocity

profiles and the location of maximum stress is located on the side of the spur dike rather than downstream as in the values derived from the measured velocity profiles (Fig. 7).

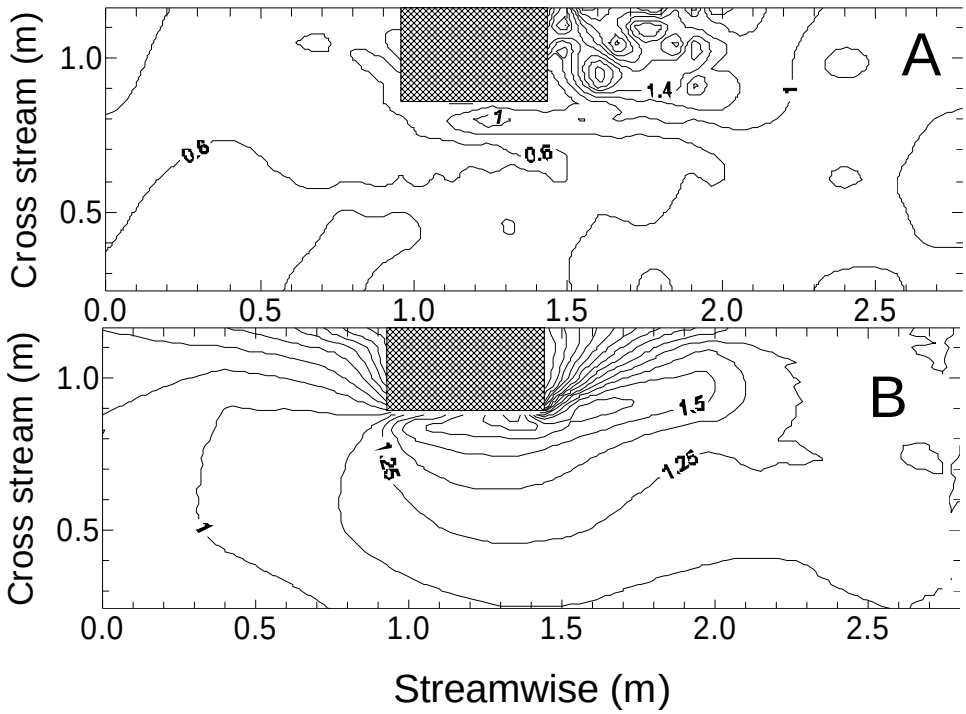

Figure 7. a) Contours of normalized bed shear stress derived from Reynolds-stress distribution near the bed for the fixed flat bed experiments. b) Contours of normalized bed shear stress derived from 3-D flow simulation. The bed shear stresses were normalized by the critical shear stress of the bed material sediment.

6. CONCLUSIONS

Three dimensional flow measurements around a model spur dike with a stationary bed were measured at 50 Hz using an ADV and compared to simulated velocities from a three-dimensional finite element model (CCHE3D). The overall agreement between the simulated and measured velocities was good, with the exception of a systematic discrepancy in areas where the *x* and *z* velocity components are negative. This occurs primarily downstream of the spur dike in the recirculation zone.

Shear stress distributions derived from both measured and simulated values correctly predicted that a scour zone downstream of the structure in the recirculation zone would form. Previous experiments with a live bed have shown this region to be one of the two sites of major scour adjacent to the spur dike. Neither shear stress distribution would predict scour at the upstream outside corner of the spur dike. Bed shear stress values derived from measured and simulated flow velocities considered in this study apparently did not contain enough information to predict the upstream scour zone observed in movable bed experiments with a similar flow.

ACKNOWLEDGEMENTS

This work is a result of research supported in part by the USDA Agriculture Research Service under the Specific Research Agreement No. 58-6408-7-035 monitored by the USDA-ARS National

Sedimentation Laboratory (NSL) and The University of Mississippi (UM). John Cox (NSL) and Emery Sayre (UM) carried out the flume measurements, and John Cox performed the initial processing of the velocity data. T.T. Zhu (UM) helped to produce many of the figures.

REFERENCES

Copeland, R. R., (1983). "Bank protection techniques using spur dikes." Miscellaneous Paper HL-83-1, U. S. Army Waterways Experiment Station, Vicksburg, Mississippi, 32 pp.

Graf, W.H., and Yulistiyanto, B., (1998). "Experiments on flow around a cylinder; the velocity and vorticity fields", Journal of Hydraulic Research, IAHR, 36(4), 637-653.

Istiyato, I., Graf, W.H., (2001). "Experiments on flow around a cylinder in a scoured channel bed", International Journal of Sediment Research, 16, (4), 431-444.

Jia, Y., and Wang, S.S.Y., (1996). "A modeling approach to predict local scour around spur dike-like structures", Proceedings of the Sixth Federal Interagency Sedimentation Conference, p. II-90-97.

Jia, Y., and Wang, S.S.Y., (1999). "Simulation of horse-shoe vortex around a bridge pier", Proceedings of the International Water Resources Engineering Conference". CD-ROM, 10 p.

Jia, Y., and Wang, S.S.Y., (2000). **"**Numerical Study of Turbulent Flow around Submerged Spur Dikes", 4th International Conference for Hydroscience and Engineering, 2000, Seoul, Korea.

Jia, Y., Kitamura, T., and Wang, S.S.Y., (2001). "Simulation scour process in a plunge pool with loose material", ASCE, *Journal of Hydraulic Engineering*, 127(3), 219-229.

Kuhnle, R., Alonso, C.V., and Shields, F.D., (1997). "Geometry of scour holes around spur dikes, and experimental study", Wang, S.S.Y., Langendoen, E.J., and Shields, F.D., (ed.) Proceedings of the Conference on Management of Landscapes Disturbed by Channel Incision, Center for Computational Hydroscience and Engineering, School of Engineering, The University of Mississippi, p. 283-287.

Kuhnle, R., Alonso, C.V., and Shields, F.D., (1999)."Geometry of scour holes associated with 90^{o} spur dikes", Journal of Hydraulic Engineering, ASCE, 125(9), 972-978.

Kwan, T.F., and Melville, B.W., (1994). "Local scour and flow measurements at bridge abutments", Journal of Hydraulic Research, IAHR, 32(5), 661-673.

Melville, B.M., and Raudkivi, A., (1977). "Flow characteristics in local scour at bridge piers", Journal of Hydraulic Research, IAHR, 15(4), 373-380.

Miller, M.C., McCave, I.N., and Komar, P.D., (1977). "Threshold of sediment motion under unidirectional currents." Sedimentology, v.24, p.507-527.

Rajaratnam, N., and Nwachukwu, B. A. (1983). "Flow near groin-like structures." Journal of Hydraulic Engineering, ASCE, 109(3), 463-480.

Richardson, J.E., and Punchang, V.G., (1998). "Three dimensional simulation of scour-induced flow at bridge piers", Journal of Hydraulic Engineering, ASCE, 124(5), 530-540.

Shields, F. D., Jr., Cooper, C. M., Knight, S. S., (1995). "Experiment in stream restoration." Journal of Hydraulic Engineering, ASCE, 121(6), 494-502.

van Rijn, L. C., (1993). "Principles of Sediment Transport in Rivers, Estuaries, and Coastal Seas". Aqua Publications, 8300AA, Emmeloord, The Netherlands.